ISSN 1063-7761, Journal of Experimental and Theoretical Physics, 2021, Vol. 133, No. 3, pp. 351–359. © Pleiades Publishing, Inc., 2021.
Russian Text © The Author(s), 2021, published in Zhurnal Eksperimental'noi i Teoreticheskoi Fiziki, 2021, Vol. 160, No. 3, pp. 415–425.

ORDER, DISORDER, AND PHASE TRANSITION IN CONDENSED SYSTEM

The Origin of an Inflection Point on the Temperature Dependence of the London Penetration Depth in Hole-Doped Cuprate High-Temperature Superconductors

K. K. Komarov[a],* and D. M. Dzebisashvili[a],**

[a] *Kirensky Institute of Physics, Siberian Branch, Russian Academy of Sciences, Krasnoyarsk, 660036 Russia*

**e-mail: constlike@gmail.com*

***e-mail: ddm@iph.krasn.ru*

Received April 1, 2021; revised April 20, 2021; accepted April 20, 2021

Abstract—A scenario of the formation of an experimentally observed inflection point on the temperature dependence of the London penetration depth λ in cuprate high-temperature superconductors (HTSCs) with optimal hole doping is discussed within the spin-polaron concept. It is shown that the reason for the appearance of an inflection point on the $1/\lambda^2(T)$ dependence is due to the features of the energy spectrum of spin-polaron quasiparticles in the superconducting phase, as well as to the specific temperature dependence of their spectral density.

DOI: 10.1134/S1063776121080021

1. INTRODUCTION

Experiments on the measurement of the temperature dependence of the magnetic field penetration depth (or the London depth) λ provide important information about the symmetry of the superconducting order parameter. The possibility to extract information on the structure of the superconducting gap on the basis of such measurements is due to the fact that the nature of the temperature evolution of the London depth is mainly determined by the density of quasiparticle states available for thermal excitation.

In particular, the temperature dependence of $1/\lambda^2$ obtained in [1] for single-crystal $YBa_2Cu_3O_{7-\delta}$ exhibits a pronounced linear behavior at low temperatures and is characterized by a finite slope at $T = 0$. This behavior of the function $1/\lambda^2(T)$ is explained by the presence of zeros in the spectrum of Bogolyubov excitations at the k-space points located at the intersection of the Fermi surface and the zero line of the d-wave order parameter and significantly differs from the well-known dependence $1/\lambda^2(T)$, which is observed in conventional superconductors with s-wave symmetry of the order parameter and is perfectly described within the BCS theory [2, 3].

The linear behavior of the function $1/\lambda^2(T)$ in the initial region is observed in many known cuprate high-temperature superconductors (HTSCs) [4–18] and is traditionally considered as evidence of the d-wave symmetry of the order parameter in these compounds.

Another interesting feature observed in the temperature dependence of $1/\lambda^2$ in some cuprate HTSCs is associated with the so-called inflection point. This point is determined by the value of temperature T_i in the vicinity of which the curve $1/\lambda^2(T)$ changes its curvature. The fact that the inflection point is not observed in all cuprates is apparently due to the choice of the measurement technique and the quality of samples [10]. For example, the inflection point manifests itself only in experiments based on muon spin rotation (μSR) spectroscopy. In a fairly large number of works [8, 16, 17, 19–25] that used the μSR spectroscopy method, the inflection point was observed; however, in some experiments [26–29] carried out by the same technique, the inflection point did not show up. When studying the London depth in HTSC cuprates by other experimental methods, this feature was not detected [4, 8, 11, 14].

The description and comparison of experimental techniques used to measure the magnetic field penetration depth can be found, for example, in [30, 31] or in the above-cited publications. We note an important advantage of μSR experiments, which is that this technique allows one to directly measure the absolute values of $\lambda^{-2}(T)$ [8]. When using other, as a rule, indirect, experimental methods for measuring the London depth, the data obtained must be normalized by $1/\lambda^2$ at $T = 0$.

The inflection point is most clearly noticeable in samples the doping level of which are close to optimal. For example, in $Bi_{2.15}Sr_{1.85}CaCu_2O_{8+\delta}$ and $Bi_{2.1}Sr_{1.9}Ca_{0.85}Y_{0.15}Cu_2O_{8+\delta}$ systems investigated in [25], the inflection point on the function $1/\lambda^2$ was especially pronounced in samples doped slightly higher than the optimal level. In approximately the same doping range, the inflection point is also observed in some other cuprate compounds.

To study the stability of the inflection point to external effects, the authors of [24] performed several cooling cycles on samples, but the experimental results remained practically unchanged. At temperatures below T_i, the dependence $\lambda^{-2}(T)$ became flatter with an increase in the magnetic field [16, 29]. This suggested that the change in the curvature of the $\lambda^{-2}(T)$ dependence at the inflection point became less noticeable. A similar behavior of the function $\lambda^{-2}(T)$ was observed in [17], where measurements were carried under varying pressure. These facts suggest that the origin of an inflection point on the temperature dependence of the inverse square of the London depth is not attributed to external factors, but is internal in origin.

Several scenarios for the origin of an inflection point have been proposed. Thus, in [32], an increase in the growth rate of the superconducting current density in the $YBa_2Cu_3O_{7-\delta}$ compound upon cooling in the temperature range below T_i was attributed to the thermal depinning of Abrikosov vortices. A similar scenario was discussed in [24] when studying the London depth in the $La_{2-x}Sr_xCuO_4$ compound. However, analytical calculations performed in these works showed that an inflection point exists only for the order parameter with *s*-wave symmetry, while no inflection point was observed for the *d*-wave order parameter, which is characteristic of cuprates. Of interest are scenarios for the origin of an inflection point that suggest the coexistence of two superconducting gaps [21, 22, 33]. In [21, 22], the case of gaps with *s* and $d_{x^2-y^2}$ wave symmetry was considered, while, in [33], the authors considered the case of d_{xy}- and $d_{x^2-y^2}$-type gaps.

In this paper, we propose an alternative mechanism for the origin of an inflection point on the temperature dependence of the inverse square of the London depth in cuprate superconductors. This mechanism does not require a change in the symmetry of the superconducting order parameter and naturally follows from the analysis of the subsystem of charge carriers in the CuO_2 plane within the spin polaron concept [34, 35].

The starting point of this concept is a strong coupling between the spin and charge degrees of freedom, which is implemented in cuprates owing to the strong electron correlations and the significant amount of hybridization between the *d* states of copper ions and *p* states on oxygen ions. Within the spin-polaron approach, the spin–charge coupling is taken into account exactly, which gives rise to a Fermi quasiparticle, whose motion is strictly correlated with the dynamics of localized spins on the nearest copper ions. Such a quasiparticle is usually called a spin polaron.

The spin-polaron concept was developed on the basis of the Kondo lattice model [36–38], as well as within the spin-fermion model (SFM). In the second case, the spin-polaron approach turned out to be especially successful in describing the properties of cuprates in both the normal [39–43] and the superconducting [44, 45] *d* phase.

The authors of [46] studied the temperature dependence of the London depth in hole-doped cuprate HTSCs within the spin-polaron concept. On the curves $\lambda^{-2}(T)$ calculated in this work, they obtained an inflection point, just as in the experiment, at doping levels close to the optimal level. However, the reason for the appearance of this feature on the corresponding curves was not revealed.

In this paper, we present the results of additional analysis to clarify the nature of the inflection point. In particular, we show that the reason for the appearance of an inflection point on the $\lambda^{-2}(T)$ dependence is associated with the specific features of the Fermi spectrum of spin-polaron quasiparticles. The latter fact can be considered as an additional Justification of correctness of using the spin-polaron approach to study the properties of hole-doped copper oxide HTSCs.

The further presentation is organized as follows. In Section 2, we describe the SFM and point out the progress achieved within this model in describing the properties of cuprates in the superconducting phase. In Section 3, we formulate the SFM Hamiltonian taking into account a weak magnetic field. In this section, we also describe a method for obtaining an expression for calculating the temperature dependence of the London depth in a system of spin-polaron quasiparticles. The reason for the appearance of an inflection point on the theoretical dependence of the London depth on temperature is revealed in Section 4. In the final Section 5, we discuss the proposed scenario for the formation of an inflection point and formulate conclusions.

2. SPIN-FERMION MODEL

The most important features of the crystal structure of the CuO_2 plane and all the main types of interactions in the electron subsystem of cuprate hole-doped HTSCs are taken into account within the Emery model or the three-band *p–d* model [47–49]. The main parameters of this model are the hopping integral of holes between oxygen ions, t_{pp}; the Coulomb interaction of two holes on a copper ion, U_d; the hybridization parameter of *p* and *d* orbitals on oxygen and copper ions, t_{pd}; and the charge-transfer gap $\Delta_{pd} =$

$\varepsilon_p - \varepsilon_d$, where ε_p and ε_d are the binding energies of holes on oxygen and copper ions, respectively.

It is important to note that the quantitative relationships between these parameters, characteristic of cuprates, correspond to the regime of strong electron correlations:

$$U_d - \Delta_{pd}, \quad \Delta_{pd} \gg t_{pd} > t_{pp}.$$

The large values of the parameters U_d and Δ_{pd}, on the one hand, significantly complicate the theoretical description of the low-temperature properties of cuprates, while, on the other hand, they make it possible to integrate the high-energy degrees of freedom in the Emery model and obtain a formally simpler SFM [50–54]. It is important that the SFM, in contrast to other effective low-energy models of cuprates, such as the Hubbard model or the t–J model, takes into account the spatial separation of hole states on the copper ion and two oxygen ions in a single unit cell of the CuO_2 plane. The most important interaction in the SFM is the exchange interaction between the spin localized on the copper ion and the hole on the nearest oxygen ion. The energy of this interaction is determined by the parameter J. The same parameter describes the intensity of spin-correlated hoppings similar to three-center interactions in the t–J^* model, the importance of which for the superconducting d phase was mentioned in [55]. In addition, the SFM takes into account the superexchange interaction in the localized spin subsystem (with the exchange integral I), as well as the Coulomb interaction between holes on oxygen ions. In this work, just as the authors of the earlier papers [46, 56], we take into account the Coulomb repulsion of two holes on the same oxygen ion with interaction energy U_p, as well as the interaction of holes on different nearest (V_1) and next nearest (V_2) ions. The SFM Hamiltonian is given in the next section and takes into account additional interactions due to the inclusion of a magnetic field.

Previously, the SFM was used to construct a theory of the superconducting d phase of cuprates within the spin-polaron concept [44, 45, 57, 58]. In particular, it was shown that the Cooper instability develops in an ensemble of spin polarons, while the exchange interaction (I) between spins localized on copper ions is responsible for the effective attraction between spin-polaron quasiparticles and acts as a mechanism of high-temperature superconductivity.

The aim of this work is to analyze the expression for the magnetic field penetration depth obtained within linear response theory on the basis of the SFM Hamiltonian and the spin-polaron concept. The procedure for obtaining an expression for $\lambda^{-2}(T)$ is described in detail in [46]. Therefore, in the next section, following this work, we only briefly describe the main steps of obtaining the expression for the London depth.

3. CALCULATION OF THE RESPONSE FUNCTION IN THE ENSEMBLE OF SPIN POLARONS

The response of spin-polaron quasiparticles to a weak magnetic field can be calculated within the Londons theory, which takes into account the relationship between the superconducting current density $\mathbf{j}$ and the vector potential of the magnetic field $\mathbf{A}$ in the local approximation:

$$\mathbf{j} = -\frac{c}{4\pi\lambda^2}\mathbf{A},$$

where c is the velocity of light. The applicability condition for the Londons theory is the relation $\lambda \gg \xi_L$, where ξ_L is the coherence length of Cooper pairs. For cuprate HTSCs, this condition is satisfied, since $\lambda \approx$ 2540 Å and $\xi_L \approx 250$ Å in these superconductors (see, for example, the review [59]). The local character of the Londons equation allows us to consider the vector potential in the long-wavelength limit ($\mathbf{A} = \mathbf{A}_{\mathbf{q}=0}$) and assume that the quantity $\mathbf{A}_{\mathbf{q}=0}$ is small.

To calculate the superconducting current $\mathbf{j}$, it is necessary to generalize the SFM Hamiltonian by including the vector potential $\mathbf{A}$, using, for example, the Peierls substitution [60, 61]. The substitution consists in the renormalization of the hopping integrals of holes (both between oxygen and copper ions and only between oxygen ions) by the phase factor

$$\exp\left\{\frac{ie}{c\hbar}\int_{R_{j'}}^{R_j} d\mathbf{r}\mathbf{A}(\mathbf{r})\right\} \cong \exp\left\{\frac{ie}{c\hbar}R_{jj'}\mathbf{A}_{\mathbf{q}=0}\right\},$$

where R_j is the radius vector of the oxygen ion with index j, $R_{jj'} = R_j - R_{j'}$, and e is the hole charge.

Within the framework of the traditional approach [2, 3, 62, 63], it is customary to expand the exponential factors in a series in a small quantity, the vector potential, up to the second order in $\mathbf{A}_{\mathbf{q}=0}$, which, in particular, makes it possible to separately analyze the paramagnetic and diamagnetic parts of the total superconducting current.

However, when using the Zwanzig–Mori projection technique [64, 65] (within the framework of which the spin-polaron concept is implemented in the above-cited papers), this approach leads to difficulties associated with the appearance of new operators that are not included in the original basis. This circumstance does not allow one to obtain an expression for the superconducting current $\mathbf{j}$ ($\mathbf{q} = 0$), closed with respect to the initial set of operators, without expanding the basis. The solution to this problem proposed in [46] was that, after the Peierls substitution, one should not try to immediately distinguish the linear and quadratic corrections in $\mathbf{A}_{\mathbf{q}=0}$, but keep the vector potential in the exponent. It turns out that this approach only slightly changes the definitions of the basis operators, but their total number does not increase. In addition, due to the holding the vector $\mathbf{A}_{\mathbf{q}=0}$ in the

exponent, followed by the transition to the quasimomentum representation, the SFM Hamiltonian takes an especially convenient form [44]:

$$\hat{H}_{\text{sp-}f} = \sum_{k\alpha}(\xi_{k,x}a^{\dagger}_{k\alpha}a_{k\alpha} + \xi_{k,y}b^{\dagger}_{k\alpha}b_{k\alpha} + \Gamma_k(a^{\dagger}_{k\alpha}b_{k\alpha} + b^{\dagger}_{k\alpha}a_{k\alpha})) + J\sum_{k\alpha}u^{\dagger}_{k\alpha}L_{k\alpha} + \frac{I}{2}\sum_{f\delta}\mathbf{S}_f\cdot\mathbf{S}_{f+2\delta} + \hat{H}_C. \quad (1)$$

When writing this expression, we used the following notation:

$$\xi_{k,x(y)} = \varepsilon_p - \mu + 2\tau s^2_{k,x(y)},$$

$$\Gamma_k = (2\tau - 4t_{pp})s_{k,x}s_{k,y}, \quad L_{k\alpha} = \sum_{q\beta}\tilde{S}^{\alpha\beta}_{k-q}u_{q\beta},$$

$$\tilde{S}_k = \frac{1}{N}\sum_f \exp(-ikS_f)(\mathbf{S}_f\cdot\boldsymbol{\sigma}), \quad (2)$$

$$u_{k\alpha} = s_{k,x}a_{k\alpha} + s_{k,y}b_{k\alpha},$$

$$s_{k,x} = \sin(k_x/2 - \alpha_x), \quad s_{k,y} = \sin(k_y/2),$$

where μ is the chemical potential, τ is the rate of hole hopping due to hybridization processes in the original Emery model in the second order of perturbation theory, N is the number of unit cells in the CuO_2 plane, $\boldsymbol{\sigma} = (\sigma^x, \sigma^y, \sigma^z)$ is a vector composed of the Pauli matrices σ^i ($i = x, y, z$), and $\mathbf{S}_f$ is the vector spin operator on a copper ion. The functions $s_{k,\,x(y)}$ arise in the transition to the k-representation and, along with the symmetry of the CuO_2-plane, also take into account the relations between the phases of the p and d orbitals.

The first sum in (1) corresponds to the kinetic energy of holes arising from doping. The operators $a^{\dagger}_{k\alpha}$ ($a_{k\alpha}$) and $b^{\dagger}_{k\alpha}$ ($b_{k\alpha}$) create (annihilate) a hole in a state with quasimomentum k and spin projection $\alpha = \pm 1/2$ in the oxygen ion subsystem with p_x and p_y orbitals, respectively. In the second sum, the product of operators $u_{k\alpha}$ and $L_{k\alpha}$ describes the hole motion along oxygen ions, correlated with the spin state on the nearest copper ion. The third sum is the superexchange interaction energy operator.

The last term in (1) takes into account the Coulomb interaction energy. In the approximation used in Section 2, this energy has the form

$$\hat{H}_C = \frac{U_p}{N}\sum_{1234}(a^{\dagger}_{1\uparrow}a^{\dagger}_{2\downarrow}a_{3\downarrow}a_{4\uparrow} + (a\to b))\delta_{1+2-3-4} + \frac{4V_1}{N}\sum_{\substack{1234\\ \alpha\beta}}\phi_{3-2}a^{\dagger}_{1\alpha}b^{\dagger}_{2\beta}b_{3\beta}a_{4\alpha}\delta_{1+2-3-4} + \frac{V_2}{N}\sum_{\substack{1234\\ \alpha\beta}}(\theta^{xy}_{2-3}a^{\dagger}_{1\alpha}a^{\dagger}_{2\beta}a_{3\beta}a_{4\alpha} + \theta^{yx}_{2-3}(a\to b))\delta_{1+2-3-4}, \quad (3)$$

where the functions

$$\theta^{xy(yx)}_k = \exp(ik_{x(y)}) + \exp(-ik_{y(x)}), \quad \phi_k = \cos(k_x/2)\cos(k_y/2) \quad (4)$$

appeared similar to the functions $s_{k,\,x(y)}$ upon passing to the quasimomentum representation and take into account the symmetry of the CuO_2 plane. For simplicity, the numbers in expression (3) denote quasimomenta the conservation law of which is provided by the Kronecker symbols $\delta_{1+2-3-4}$.

The above-mentioned convenience of writing the SFM Hamiltonian in the form (1) is due to the fact that the dependence on the field of the vector potential $\mathbf{A}_{\mathbf{q}=0}$, the direction of which is chosen along the x axis, manifests itself only in the phase shift in the argument of the trigonometric function $s_{k,\,x}$. The value of the shift α_x is given by the expression

$$\alpha_x = \frac{eg_x}{2c\hbar}A^x_{\mathbf{q}=0}, \quad (5)$$

where g_x is the unit cell parameter along the x axis.

The Zeeman energy due to the interaction of the field with the hole spins is not taken into account in Hamiltonian (1), since this energy vanishes in the long-wavelength limit ($\mathbf{q}\to 0$).

We used the following numerical values (in eV) for the SFM parameters:

$$\tau = 0.1, \quad J = 3.4, \quad I = 0.136\ [66],$$

$$t_{pp} = 0.11\ [43, 67], \quad U_p = 4.0\ [68, 69],$$

$$V_1 = 1.5\ [70], \quad V_2 = 0.12\ [71].$$

We will not dwell on the discussion of the values of these parameters, since this issue has been considered in detail in the relevant cited works. We only note that, according to the results of [67], the parameter V_1, which corresponds to the intensity of the Coulomb interaction of holes on the nearest oxygen ions, does not affect the value of T_c, since it drops out from the system of equations for the d-wave order parameter for symmetry reasons.

The expression for the superconducting current density is obtained, as usual [61], by varying the Hamiltonian over the vector potential field, followed by averaging over the thermodynamic ensemble. Moreover, the density matrix with which the averaging is performed must take into account the field $\mathbf{A}_{\mathbf{q}=0}$. As a result, the expression for the superconducting current density is obtained in the form

$$j_x(\mathbf{q}=0) = \frac{eg_x}{\hbar}\sum_{k\alpha}\cos\left(\frac{k_x}{2} - \alpha_x\right)(2\tau s_{k,x}\langle a^{\dagger}_{k\alpha}a_{k\alpha}\rangle + 2(\tau - 2t_{pp})s_{k,y}\langle a^{\dagger}_{k\alpha}b_{k\alpha}\rangle + J\langle a^{\dagger}_{k\alpha}L_{k\alpha}\rangle), \quad (6)$$

where the dependence on the field of the vector potential $A^x_{\mathbf{q}=0}$ is defined only as an additive renormalization

of the quasimomentum k_x by the value α_x. This renormalization in formula (6) is taken into account both explicitly, in the argument of the cosine and in the function $s_{k,\,x}$, and implicitly, in the thermodynamic averages.

Note that expression (6) gives the correct limiting behavior of the superconducting current density during the transition to the normal phase. As shown in [46], in the limit as $T \to T_c$, the right-hand side of (6) identically vanishes, as it should be.

The expression for the magnetic field penetration depth follows from the Londons equation

$$\mathbf{j} = -\frac{c}{4\pi\lambda^2}\mathbf{A}$$

and has the form

$$\frac{1}{\lambda^2} = -\frac{2e\pi}{c^2\hbar g_y g_z}\frac{j_x(\mathbf{q}=0)}{N\alpha_x}, \qquad (7)$$

where $g_{y(z)}$ is the lattice parameter along the $y(z)$ axis and the current density j_x ($\mathbf{q} = 0$) is determined by expression (6).

Since the values of λ^{-2} must be calculated by formula (7) in the limit as $A^x_{\mathbf{q}=0} \to 0$, the second fraction on the right-hand side of (7) is, up to a constant, simply the derivative of the current density with respect to the vector potential at the point $A^x_{\mathbf{q}=0} = 0$. This means that, when determining the London depth, only corrections linear in $A^x_{\mathbf{q}=0}$ to the current density j_x ($\mathbf{q} = 0$) are actually taken into account, as it should be in linear response theory.

The explicit dependence of the current density on the vector potential, due to the projection method used, turns out to be rather complicated. Despite the fact that the analytical calculation of the derivative of the current density with respect to α_x is, in principle, possible, a simpler solution is numerical differentiation. In this case, of course, the values of α_x should be taken from the interval in which the function $j_x(\alpha_x)$ is linear [46].

4. THE ORIGIN OF AN INFLECTION POINT ON THE TEMPERATURE DEPENDENCE OF THE LONDON DEPTH

A significant factor for calculating the current density is the fact that only three operators appear in formula (6) in the definition of thermodynamic averages: $a_{k\alpha}$, $b_{k\alpha}$, and $L_{k\alpha}$; it is these operators that are used in the definition of the SFM Hamiltonian (1). If the corresponding exponents in Hamiltonian (1) were expanded to the second order in the potential $A^x_{\mathbf{q}=0}$, as is customary, then an additional composite operator of the form

$$\sum_{q\beta}\tilde{S}^{\alpha\beta}_{k-q}\left[\cos\left(\frac{q_x}{2}\right)a_{q\beta} + s_{q,y}b_{q\beta}\right],$$

would appear in the expression for the current, which, obviously, does not reduce to a linear combination of the original three operators $a_{k\alpha}$, $b_{k\alpha}$, and $L_{k\alpha}$.

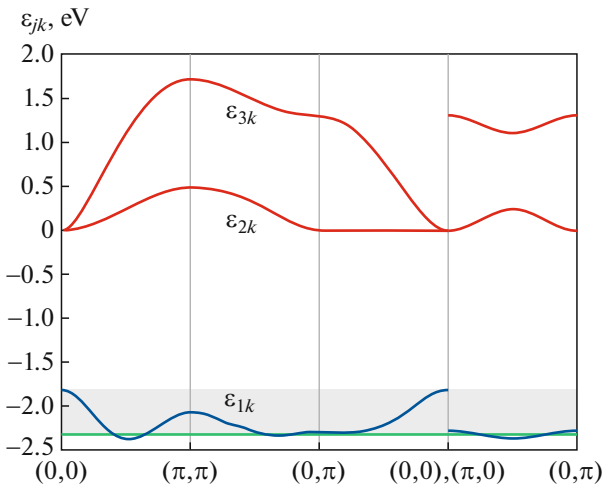

Fig. 1. SFM spectrum of Fermi excitations in the normal phase. The lower band ε_{1k} corresponds to spin-polaron states (blue curves) formed due to the strong spin-fermion coupling J. The upper bands ε_{2k} and ε_{3k} are mainly formed by purely hole states. In the low-density regime, when the chemical potential (green line) lies in the lower spin-polaron band, these bands remain empty. A specific feature of the spin-polaron spectrum is that it has a minimum in the vicinity of the points $(\pm\pi/2, \pm\pi/2)$ [43, 72].

Thus, within the proposed scheme for calculating the superconducting current density, six operators can be considered as basis operators. The first three are the operators $a_{k\uparrow}$, $b_{k\uparrow}$, and $L_{k\uparrow}$. The basis of these operators is sufficient for a satisfactory description of, for example, the spectral properties of cuprates in the normal phase (see Fig. 1). It should be noted here that the operator $L_{k\alpha}$ is extremely important. The inclusion of precisely $L_{k\alpha}$ in the basis allows us to correctly take into account the strong coupling between a spin localized on a copper ion and a hole moving along the four nearest oxygen ions [42]. To describe the anomalous properties of an ensemble of spin polarons, it is necessary to add three more operators, $a^\dagger_{-k\downarrow}$, $b^\dagger_{-k\downarrow}$, and $L^\dagger_{-k\downarrow}$, to the operator basis [44].

In [46], we used this basis of six operators, $a_{k\uparrow}$, $b_{k\uparrow}$, $L_{k\uparrow}$, $a^\dagger_{-k\downarrow}$, $b^\dagger_{-k\downarrow}$, and $L^\dagger_{-k\downarrow}$, to calculate the thermodynamic averages appearing in expression (6) for the superconducting current. The calculation was carried out within the Zwanzig–Mori projection method [64, 65], on the basis of which the spin-polaron concept

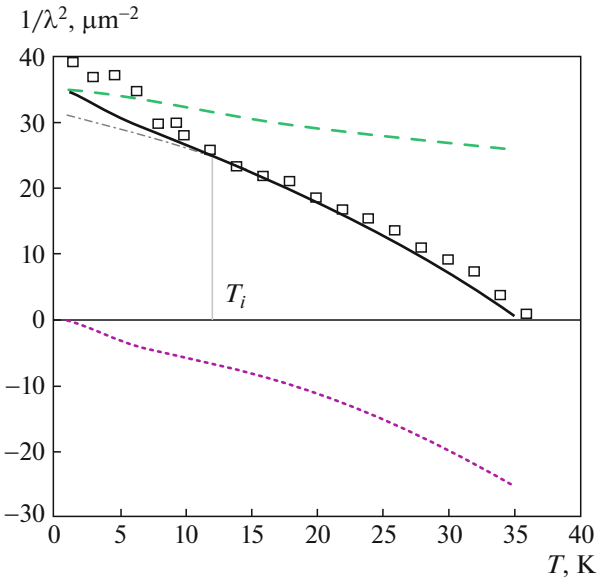

Fig. 2. Inflection point on the experimental and theoretical temperature dependence of the inverse square of the London depth at $x = 0.17$. The solid curve is calculated in the spin-polaron approach, and the symbols represent experimental data for $La_{1.83}Sr_{0.17}CuO_4$ [21, 24]. The dash-dotted line for $T < T_i$ is the extrapolation of the function $\lambda^{-2}(T)$ on the right of the inflection point T_i. The lower dashed curve demonstrates the temperature dependence of the term (8) selected from the right-hand side of expression (7) for λ^{-2}. The upper dashed curve reflects the sum of the remaining terms on the right-hand side of (7). The sum of the dotted and dashed curves is given by the solid curve. The model parameters (in eV) are as follows: $J = 3.4$, $\tau = 0.1$, $I = 0.136$, $t_{pp} = 0.11$, $U_p = 4.0$, and $V_2 = 0.12$.

was implemented in the previous works [39, 42]. By calculating the thermodynamic averages in (6) and substituting the result for the current into (7), we found an expression for the inverse square of the penetration depth. Due to the awkwardness of this expression, we do not reproduce it in full here; but below we give a part of this expression that will be necessary for our purposes.

An example of the function $\lambda^{-2}(T)$ obtained in [46] for a doping value of $x = 0.17$ on the basis of self-consistent numerical calculations of the equation for j_x ($\mathbf{q} = 0$) (jointly with the equation for the order parameter and the chemical potential) is shown by the solid curve in Fig. 2. An important result of these numerical calculations is that an inflection point is observed on the theoretical dependence $\lambda^{-2}(T)$, which fairly well reproduces a similar feature in the experimental dependence shown in the same Fig. 2 by square symbols. However, the physical reason for the appearance of the inflection point on the theoretical curves was not revealed in the cited papers.

As follows from expression (7), to answer this question, one should take the derivative of a rather complicated expression for the current j_x ($\mathbf{q} = 0$) obtained earlier in [46] with respect to the phase α_x. As a result, a large set of terms arises each of which should be analyzed. Fortunately, there is no need to write out all these terms here, because, as numerical analysis has shown, only one of them leads to an inflection point on the $1/\lambda^2(T)$ curve. This term has the form

$$\frac{3\pi g_x e^2}{\hbar g_y g_z c^2} J^2(\varepsilon_p - \mu)\frac{1}{N} \times \sum_k \frac{f'(E_k/T)\sin(k_x)\varepsilon_{2k}\varepsilon_{3k}}{(E_k^2 - \varepsilon_{2k}^2)(E_k^2 - \varepsilon_{3k}^2)} v_{k,x}^{s-p}. \quad (8)$$

Here the prime at the Fermi–Dirac distribution function $f(x) = (e^x + 1)^{-1}$ denotes its derivative with respect to the energy $E_k = \sqrt{(\varepsilon_{1k} - \mu)^2 + |\Delta_k|^2}$ of Bogolyubov excitations, where $|\Delta_k|^2$ is the gap function of $d_{x^2-y^2}$-wave symmetry [73] and T is temperature. Three branches of the spectrum ε_{jk} ($j = 1, 2, 3$) describe the band structure of spin-polaron quasiparticles in the normal phase (see Fig. 1). Here $v_{k,x}^{s-p}$ denotes the projection of the velocity of spin-polaron quasiparticles onto the x axis:

$$v_{k,x}^{s-p} = \frac{1}{\hbar}\frac{d\varepsilon_{1k}}{dk_x}. \quad (9)$$

In Fig. 2, the lower dashed curve represents the temperature dependence of the term (8),which is extracted from the general expression for λ^{-2}; the full expression is given in [46]. In the vicinity of 12 K, this curve exhibits a change in curvature corresponding to the inflection point. The upper dashed line shows the temperature dependence of all the other contributions that remained in the expression for λ^{-2} after separating the term (8). One can see that the temperature dependence of these contributions does not show any features indicating the presence of an inflection point. The solid line in Fig. 2 is the sum of the dotted and dashed lines and describes, as mentioned above, the temperature dependence of the inverse square of the London depth at a doping level of $x = 0.17$. Thus, we see that the presence of an inflection point on the resulting curve $\lambda^{-2}(T)$ is attributed solely to the term (8).

The analysis of the structure of expression (8) allows us to reveal the reason for the anomalous temperature behavior of λ^{-2}. Indeed, since, at low temperatures, the derivative of the Fermi–Dirac function in (8) is proportional to the delta function, the main contribution to the sum over the quasimomenta k comes from the neighborhood of points of the Brillouin zone where E_k vanishes, that is, at the intersection of the Fermi surface (hole pockets) and the zero

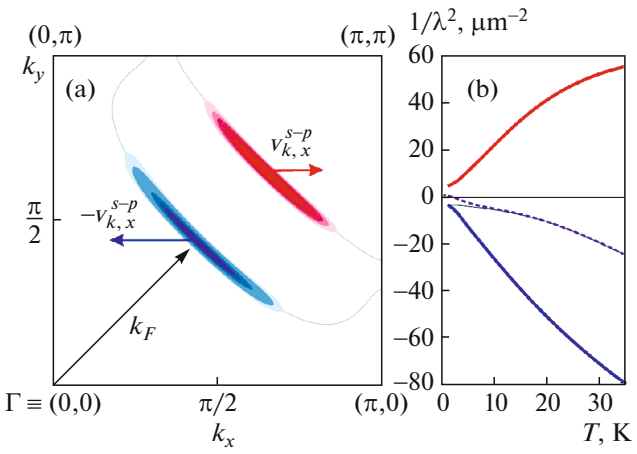

Fig. 3. The origin of an inflection point on the dependence $1/\lambda^2(T)$ within the spin-polaron concept. (a) Two neighborhoods of the intersection points of the zero line of the order parameter and the Fermi surface in the first quadrant of the Brillouin zone are shown in blue and red (the doping level is $x = 0.17$ and $T = 20$ K); the projections of quasiparticle velocities on the horizontal axis for the red region are opposite in sign to the corresponding projections of quasiparticle velocities for the blue region. (b) Contributions to the temperature dependence of (8) from the red and blue regions of the Brillouin zone are marked in red and blue, respectively; competition between these two contributions ultimately gives rise to an inflection point on the temperature dependence $\lambda^{-2}(T)$ shown by the solid line in Fig. 2 and by the dashed line in Fig. 3b. The model parameters are the same as in Fig. 2.

lines of the *d*-wave order parameter. There are two such points in each quadrant of the Brillouin zone. In Fig. 3a, the neighborhoods of these points are highlighted in blue and red.

An important circumstance for explaining the appearance of an inflection point on the $1/\lambda^2(T)$ curve is that the group velocities of Fermi quasiparticles in these two regions have opposite signs. Therefore, the contributions from the red and blue regions to the sum in expression (8) turn out to be opposite in sign. Separate contributions from the red and blue regions (which increase in area with increasing temperature) to the sum (8) as a function of temperature are shown in Fig. 3b by red and blue lines, respectively. The contribution from the blue region (which is located closer to the Γ point of the Brillouin zone) is negative, and its temperature dependence is concave downward. The contribution from the red region (which is located farther from the Γ point) is, on the contrary, positive, and its temperature dependence is concave upward. As a result of competition between the contributions from these two regions to the sum (8), an inflection point arises on the resulting dependence $1/\lambda^2(T)$ shown by the solid line in Fig. 2.

5. DISCUSSION AND CONCLUSIONS

The analysis carried out within the spin-polaron concept has shown that the origin of an inflection point on the temperature dependence of the inverse square of the London depth in cuprate HTSCs is attributed to the specific features of the spectrum of spin-polaron quasiparticles associated with the presence of two intersection points of the Fermi surface with the zero line of the *d*-wave order parameter in each quadrant of the Brillouin zone.

Not only the fact that the states of Fermi spin-polaron quasiparticles at the two above-mentioned intersection points gives a competing (in sign) contribution to the expression for $1/\lambda^2$, but also the fact that the nature of the temperature dependence of these contributions is different (see Fig. 3b), are important for the appearance of an inflection point. The temperature dependence of the contribution of the states from the neighborhood nearest to the Γ point of the Brillouin zone (the blue region in Fig. 3a) has a downward concave shape, whereas the temperature dependence of the contributions from the neighborhood distant from the Γ point (the red region in Fig. 3a) is concave upward. The latter fact is due to the different temperature dependence of the spectral weight of quasiparticles from these two neighborhoods of the intersection points of the Fermi surface with the zero line of the order parameter. Obviously, the specific character of this dependence is due to the spin-polaron nature of Fermi quasiparticles.

In this work, we have carried out an analysis of the reason for the origin of an inflection point on the temperature dependence of the London depth in cuprate HTSCs for a doping value of $x = 0.17$, which is close to the optimal value. The choice of this value of x has been primarily associated with the fact that it is the optimal doping region in which the inflection point is experimentally determined most clearly. On the other hand, the theoretical temperature dependence of λ^{-2} obtained in [46] agrees best with the experimental curves for the values of x in the interval $0.12 < x < 0.2$, which includes the optimal doping region. At the same time, with an increase in the doping level, the inflection point shifts to lower temperatures, while, with a decrease in x, it shifts to higher T. Outside the interval $0.12 < x < 0.2$, the agreement with experiment worsens, in our view, for the following reasons: for the values of $x > 0.2$, the low density approximation used in this work is insufficient, while, for $x < 0.12$, the pseudogap effects, which are not taken into account in this theory, become important.

We should also make the following remark regarding the topology of the Fermi surface. The representation of the Fermi surface in weakly doped cuprate HTSCs in the form of four hole pockets centered in the vicinity of the points $(\pm\pi/2, \pm\pi/2)$ of the Brillouin zone is the result of numerical calculations that are largely based on model Hamiltonians. Experimen-

tally, one observes only the edge of the hole pocket close to the Γ point of the Brillouin zone—the so-called Fermi arcs (the blue region in Fig. 3a). The far edge of the hole pocket (the red region in Fig. 3a) is usually (for example, in ARPES experiments [74, 75]) invisible. It is believed that the spectral weight of these states is significantly suppressed due to significant spin fluctuation scattering [76, 77]. Obviously, the suppression of the spectral weight of the states corresponding to the red region leads to a decrease in their contribution to expression (8) for $1/\lambda^2$ and, accordingly, to an increase in the relative contribution of the states from the blue region. The comparison of the corresponding curves in Fig. 3b shows that this should lead to an even greater slope of the resulting dependence $1/\lambda^2(T)$ in the low-temperature region; as a result, one can expect an even stronger manifestation of the inflection point.

Finally, note that the distinctive feature of the scenario for the appearance of an inflection point on the $1/\lambda^2(T)$ dependence, proposed in this paper, is that there is no need to modify the symmetry of the *d*-wave order parameter, for example, by adding the *s* component, as was done in [21, 22]. Within the spin-polaron approach, the inflection point appears naturally, and therefore its experimental observation can be considered as a justification of using the concept of spin-polaron quasiparticles to describe the spectral and superconducting properties of cuprate superconductors.

FUNDING

This work was supported by the Russian Foundation for Basic Research, project nos. 18-02-00837 and 20-32-70059.

REFERENCES

1. W. N. Hardy, D. A. Bonn, D. C. Morgan, R. Liang, and K. Zhang, Phys. Rev. Lett. **70**, 3999 (1993).
2. M. Tinkham, *Introduction to Superconductivity* (Courier, North Chelmsford, MA, 2004).
3. J. R. Schrieffer, *Theory of Superconductivity* (CRC, Boca Raton, FL, 2018).
4. T. Jacobs, S. Sridhar, Qiang Li, G. D. Gu, and N. Koshizuka, Phys. Rev. Lett. **75**, 4516 (1995).
5. C. Panagopoulos, J. R. Cooper, G. B. Peacock, I. Gameson, P. P. Edwards, W. Schmidbauer, and J. W. Hodby, Phys. Rev. B **53**, 2999(R) (1996).
6. D. M. Broun, D. C. Morgan, R. J. Ormeno, S. F. Lee, A. W. Tyler, A. P. Mackenzie, and J. R. Waldram, Phys. Rev. B **56**, 11443(R) (1997).
7. C. Panagopoulos, J. R. Cooper, and T. Xiang, Phys. Rev. B **57**, 13422 (1998).
8. C. Panagopoulos, B. D. Rainford, J. R. Cooper, W. Lo, J. L. Tallon, J. W. Loram, J. Betouras, Y. S. Wang, and C. W. Chu, Phys. Rev. B **60**, 14617 (1999).
9. R. F. Wang, S. P. Zhao, G. H. Chen, and Q. S. Yang, Appl. Phys. Lett. **75**, 3865 (1999).
10. K. M. Paget, S. Guha, M. Z. Cieplak, I. E. Trofimov, S. J. Turneaure, and T. R. Lemberger, Phys. Rev. B **59**, 641 (1999).
11. A. Hosseini, R. Harris, S. Kamal, P. Dosanjh, J. Preston, R. Liang, W. N. Hardy, and D. A. Bonn, Phys. Rev. B **60**, 1349 (1999).
12. D. M. Broun, W. A. Huttema, P. J. Turner, S. Özcan, B. Morgan, R. Liang, W. N. Hardy, and D. A. Bonn, Phys. Rev. Lett. **99**, 237003 (2007).
13. T. R. Lemberger, I. Hetel, A. Tsukada, and M. Naito, Phys. Rev. B **82**, 214513 (2010).
14. T. R. Lemberger, I. Hetel, A. Tsukada, M. Naito, and M. Randeria, Phys. Rev. B 83, 140507(R) (2011).
15. A. V. Pronin, T. Fischer, J. Wosnitza, A. Ikeda, and M. Naito, Phys. C **473**, 11 (2012).
16. J. E. Sonier, J. Phys. Soc. Jpn. **85**, 091005 (2016).
17. Z. Guguchia, R. Khasanov, A. Shengelaya, E. Pomjakushina, S. J. L. Billinge, A. Amato, E. Morenzoni, and H. Keller, Phys. Rev. B **94**, 214511 (2016).
18. I. Božović, X. He, J. Wu, and A. T. Bollinger, Nature (London, U.K.) **536**, 309 (2016).
19. J. E. Sonier, J. H. Brewer, R. F. Kiefl, G. D. Morris, R. I. Miller, D. A. Bonn, J. Chakhalian, R. H. Heffner, W. N. Hardy, and R. Liang, Phys. Rev. Lett. **83**, 4156 (1999).
20. A. T. Savici, A. Fukaya, I. M. Gat-Malureanu, T. Ito, P. L. Russo, Y. J. Uemura, C. R. Wiebe, P. P. Kyriakou, G. J. MacDougall, M. T. Rovers, G. M. Luke, K. M. Kojima, M. Goto, S. Uchida, R. Kadono, et al., Phys. Rev. Lett. **95**, 157001 (2005).
21. R. Khasanov, A. Shengelaya, A. Maisuradze, F. la Mattina, A. Bussmann-Holder, H. Keller, and K. A. Müller, Phys. Rev. Lett. **98**, 057007 (2007).
22. R. Khasanov, S. Strässle, D. di Castro, T. Masui, S. Miyasaka, S. Tajima, A. Bussmann-Holder, and H. Keller, Phys. Rev. Lett. **99**, 237601 (2007).
23. R. Khasanov, A. Shengelaya, J. Karpinski, A. Bussmann-Holder, H. Keller, and K. A. Müller, J. Supercond. Nov. Magn. **21**, 81 (2008).
24. B. M. Wojek, S. Weyeneth, S. Bosma, E. Pomjakushina, and R. Puźniak, Phys. Rev. B **84**, 144521 (2011).
25. W. Anukool, S. Barakat, C. Panagopoulos, and J. R. Cooper, Phys. Rev. B **80**, 024516 (2009).
26. C. Bernhard, Ch. Niedermayer, U. Binninger, A. Hofer, Ch. Wenger, J. L. Tallon, G. V. M. Williams, E. J. Ansaldo, J. I. Budnick, C. E. Stronach, D. R. Noakes, and M. A. Blankson-Mills, Phys. Rev. B **52**, 10488 (1995).
27. P. Zimmermann, H. Keller, S. L. Lee, I. M. Savić, M. Warden, D. Zech, R. Cubitt, E. M. Forgan, E. Kaldis, J. Karpinski, and C. Krüger, Phys. Rev. B **52**, 541 (1995).
28. A. Suter, G. Logvenov, A. V. Boris, F. Baiutti, F. Wrobel, L. Howald, E. Stilp, Z. Salman, T. Prokscha, and B. Keimer, Phys. Rev. B **97**, 134522 (2018).
29. L. Howald, E. Stilp, F. Baiutti, C. Dietl, F. Wrobel, G. Logvenov, T. Prokscha, Z. Salman, N. Wooding, D. Pavuna, H. Keller, and A. Suter, Phys. Rev. B **97**, 094514 (2018).

30. W. N. Hardy, S. Kamal, and D. A. Bonn, *Magnetic Penetration Depths in Cuprates: A Short Review of Measurement Techniques and Results,* Vol. 371 of *NATO Science Ser. B* (Springer, Boston, MA, 2002).

31. R. Prozorov and R. W. Giannetta, Supercond. Sci. Technol. **19**, R41 (2006).

32. D. R. Harshman and A. T. Fiory, J. Phys.: Condens. Matter **23**, 315702 (2011).

33. A. Valli, G. Sangiovanni, M. Capone, and C. di Castro, Phys. Rev. B **82**, 132504 (2010).

34. A. F. Barabanov, L. A. Maksimov, and A. V. Mikheyenkov, AIP Conf. Proc. **527**, 1 (2000).

35. V. V. Val'kov, D. M. Dzebisashvili, M. M. Korovushkin, and A. F. Barabanov, Phys. Usp. **91** (2021, in press).

36. L. A. Maksimov, A. F. Barabanov, and R. O. Kuzian, Phys. Lett. A **232**, 286 (1997).

37. L. A. Maksimov, R. Hayn, and A. F. Barabanov, Phys. Lett. A **238**, 288 (1998).

38. V. V. Val'kov, M. M. Korovushkin, and A. F. Barabanov, JETP Lett. **88**, 370 (2008).

39. A. F. Barabanov, V. M. Berezovskii, E. Zhasinas, and L. A. Maksimov, J. Exp. Theor. Phys. **83**, 819 (1996).

40. A. F. Barabanov, E. Žsinas, O. V. Urazaev, and L. A. Maksimov, JETP Lett. **66**, 182 (1997).

41. R. O. Kuzian, R. Hayn, and A. F. Barabanov, Phys. Rev. B **68**, 195106 (2003).

42. A. F. Barabanov, R. Khain, A. A. Kovalev, O. V. Urazaev, and A. M. Belemuk, J. Exp. Theor. Phys. **92**, 677 (2001).

43. D. M. Dzebisashvili, V. V. Val'kov, and A. F. Barabanov, JETP Lett. **98**, 528 (2013).

44. V. V. Val'kov, D. M. Dzebisashvili, and A. F. Barabanov, Phys. Lett. A **379**, 421 (2015).

45. V. V. Val'kov, D. M. Dzebisashvili, M. M. Korovushkin, and A. F. Barabanov, J. Magn. Magn. Mater. **440**, 123 (2017).

46. D. M. Dzebisashvili and K. K. Komarov, Eur. Phys. J. B **91**, 278 (2018).

47. V. J. Emery, Phys. Rev. Lett. **58**, 2794 (1987).

48. C. M. Varma, S. Schmitt-Rink, and E. Abrahams, Solid State Commun. **62**, 681 (1987).

49. J. E. Hirsch, Phys. Rev. Lett. **59**, 228 (1987).

50. J. Zaanen and A. M. Oleś, Phys. Rev. B **37**, 9423 (1988).

51. V. J. Emery and G. Reiter, Phys. Rev. B **38**, 4547 (1988).

52. P. Prelovšek, Phys. Lett. A **126**, 287 (1988).

53. E. B. Stechel and D. R. Jennison, Phys. Rev. B **38**, 4632 (1988).

54. A. F. Barabanov, L. A. Maksimov, and G. V. Uimin, Sov. Phys. JETP **69**, 371 (1989).

55. V. V. Val'kov, T. A. Val'kova, D. M. Dzebisashvili, and S. G. Ovchinnikov, Mod. Phys. Lett. B **17**, 441 (2003).

56. K. K. Komarov and D. M. Dzebisashvili, Phys. Scr. **95**, 065806 (2020).

57. V. V. Val'kov, D. M. Dzebisashvili, and A. F. Barabanov, J. Low Temp. Phys. **181**, 134 (2015).

58. V. V. Val'kov, D. M. Dzebisashvili, M. M. Korovushkin, and A. F. Barabanov, J. Exp. Theor. Phys. **125**, 810 (2017).

59. C. W. Chu, L. Z. Deng, and B. Lv, Phys. C (Amsterdam, Neth.) **514**, 290 (2015).

60. R. E. Peierls, Z. Phys. **80**, 763 (1933).

61. E. M. Lifshits and L. P. Pitaevski, *Course of Theoretical Physics,* Vol. 9: *Statistical Physics, Part 2* (Fizmatlit, Moscow, 2015; Pergamon, New York, 1980).

62. M. V. Eremin, I. A. Larionov, and I. E. Lyubin, J. Phys.: Condens. Matter **22**, 185704 (2010).

63. Zh. Huang, H. Zhao, and Sh. Feng, Phys. Rev. B **83**, 144524 (2011).

64. R. Zwanzig, Phys. Rev. **124**, 983 (1961).

65. H. Mori, Prog. Theor. Phys. **33**, 423 (1965).

66. G. Shirane, Y. Endoh, R. J. Birgeneau, M. A. Kastner, Y. Hidaka, M. Oda, M. Suzuki, and T. Murakami, Phys. Rev. Lett. **59**, 1613 (1987).

67. V. V. Val'kov, D. M. Dzebisashvili, and A. F. Barabanov, J. Supercond. Nov. Magn. **29**, 1049 (2016).

68. M. S. Hybertsen, M. Schlüter, and N. E. Christensen, Phys. Rev. B **39**, 9028 (1989).

69. A. K. McMahan, J. F. Annett, and R. M. Martin, Phys. Rev. B **10**, 6268 (1990).

70. M. H. Fischer, Phys. Rev. B **84**, 144502 (2011).

71. R. O. Zaitsev, Phys. Lett. A **134**, 199 (1988).

72. A. F. Barabanov, V. M. Beresovsky, E. Žasinas, and L. A. Maksimov, Phys. C (Amsterdam, Neth.) **252**, 308 (1995).

73. V. V. Val'kov, D. M. Dzebisashvili, and A. F. Barabanov, JETP Lett. **104**, 730 (2016).

74. A. Damascelli, Z. Hussain, and Zh.-X. Shen, Rev. Mod. Phys. **75**, 473 (2003).

75. T. Yoshida, X. J. Zhou, D. H. Lu, S. Komiya, Yo. Ando, H. Eisaki, T. Kakeshita, S. Uchida, Z. Hussain, Z.-X. Shen, and A. Fujimori, J. Phys.: Condens. Matter **19**, 125209 (2007).

76. N. Doiron-Leyraud, C. Proust, D. Le Boeuf, J. Levallois, J.-B. Bonnemaison, R. Liang, D. A. Bonn, W. N. Hardy, and L. Taillefer, Nature (London, U.K.) **447**, 565 (2007).

77. E. Razzoli, Y. Sassa, G. Drachuck, M. Mansson, A. Keren, M. Shay, M. H. Berntsen, O. Tjernberg, M. Radovic, J. Chang, S. Pailhé, N. Momono, M. Oda, M. Ido, O. J. Lipscombe, S. M. Hayden, L. Patthey, J. Mesot, and M. Shi, New J. Phys. **12**, 125003 (2010).

Translated by I. Nikitin